Available online at www.sciencedirect.com
SCIENCE DIRECT®
Journal of Biotechnology 117 (2005) 395–405
Journal of BIOTECHNOLOGY
www.elsevier.com/locate/jbiotec

Effect of different levels of NADH availability on metabolic fluxes of *Escherichia coli* chemostat cultures in defined medium

Ailen M. Sánchez [a], George N. Bennett [b], Ka-Yiu San [a,c,*]

[a] *Department of Bioengineering, Rice University, 6100 Main Street, MS-142, Houston, TX, USA*
[b] *Department of Biochemistry and Cell Biology, Rice University, Houston, TX, USA*
[c] *Department of Chemical Engineering, Rice University, Houston, TX, USA*

Received 6 September 2004; received in revised form 7 February 2005; accepted 21 February 2005

Abstract

Escherichia coli overexpressing a NAD^+-dependent formate dehydrogenase (FDH) from *Candida boidinii* was grown in chemostat culture on various carbon sources at $0.05\,h^{-1}$ dilution rate, under anaerobic conditions using defined medium and compared to a control without the heterologous FDH pathway. Metabolic fluxes, NADH/NAD^+ ratios and NAD($H/^+$) levels were determined under a range of intracellular NADH availability. The effect of NADH manipulation on the distribution of metabolic fluxes in *E. coli* was assessed under steady-state conditions.

The heterologous FDH pathway converts 1 mol of formate into 1 mol of NADH and carbon dioxide, in contrast with the native FDH where no cofactor involvement is present. Previously, we found that this NADH regeneration system doubled the maximum yield of NADH from 2 to 4 mol NADH/mol glucose consumed and reached 4.6 mol NADH/mol of substrate when sorbitol was used as a carbon source in a complex medium.

In the current study, it was found that higher NADH yields and NADH/NAD^+ ratios were achieved with our in vivo NADH regeneration system compared to a control lacking the new FDH pathway in the three carbon sources (glucose, gluconate and sorbitol) examined suggesting a more reduced intracellular environment. The total NAD($H/^+$) amounts were very similar for all the combinations studied. It was also found that the ethanol to acetate ratio increased with increased NADH availability. This ratio increased from 1.05 for the control strain in glucose to 9.45 for the strain expressing the heterologous NAD^+-dependent FDH in sorbitol.

Keywords: Chemostat culture; Formate dehydrogenase; Metabolic fluxes; NADH; *Escherichia coli*

1. Introduction

Under anaerobic growth, and in the absence of an alternate oxidizing agent, the regeneration of NAD^+ is achieved through fermentation by using NADH

* Corresponding author. Tel.: +1 713 348 5361; fax: +1 713 348 5877.
E-mail address: ksan@rice.edu (K.-Y. San).

0168-1656/$ – see front matter © 2005 Elsevier B.V. All rights reserved.
doi:10.1016/j.jbiotec.2005.02.006

to reduce metabolic intermediates (Clark, 1989; De Graef et al., 1999) (Fig. 1). Therefore, in fermentation, alterations in the availability of NADH should have a profound effect in the whole metabolic network.

Our previous studies established cofactor manipulations for the NADH/NAD^+ cofactor pair as an additional tool for metabolic engineering. We investigated different external and genetic means of increasing the availability of NADH and examined the effect of these manipulations on the distribution of metabolites in *Escherichia coli*. The strategies included feeding carbon sources with different oxidation states (Alam and Clark, 1989; San et al., 2002; Berríos-Rivera, 2002a), overexpressing an enzyme that can regenerate NADH (Berríos-Rivera et al., 2002b,c), overexpressing an enzyme in the NAD salvage pathway (NAPRTase; *pncB*) (Berríos-Rivera et al., 2002d), eliminating NADH competing pathways (Berríos-Rivera et al., 2003) and varying the NADH availability by combining external and genetic means, i.e., feeding different carbons sources with different oxidation states to an *E. coli* strain overexpressing an NAD^+-dependent FDH thus achieving a range of NADH availability in anaerobic tube experiments (Berríos-Rivera et al., 2004).

In previous studies (Berríos-Rivera et al., 2002b,c, 2004), we increased the availability of intracellular NADH in vivo by regenerating NADH through the heterologous expression of a NAD^+-dependent formate

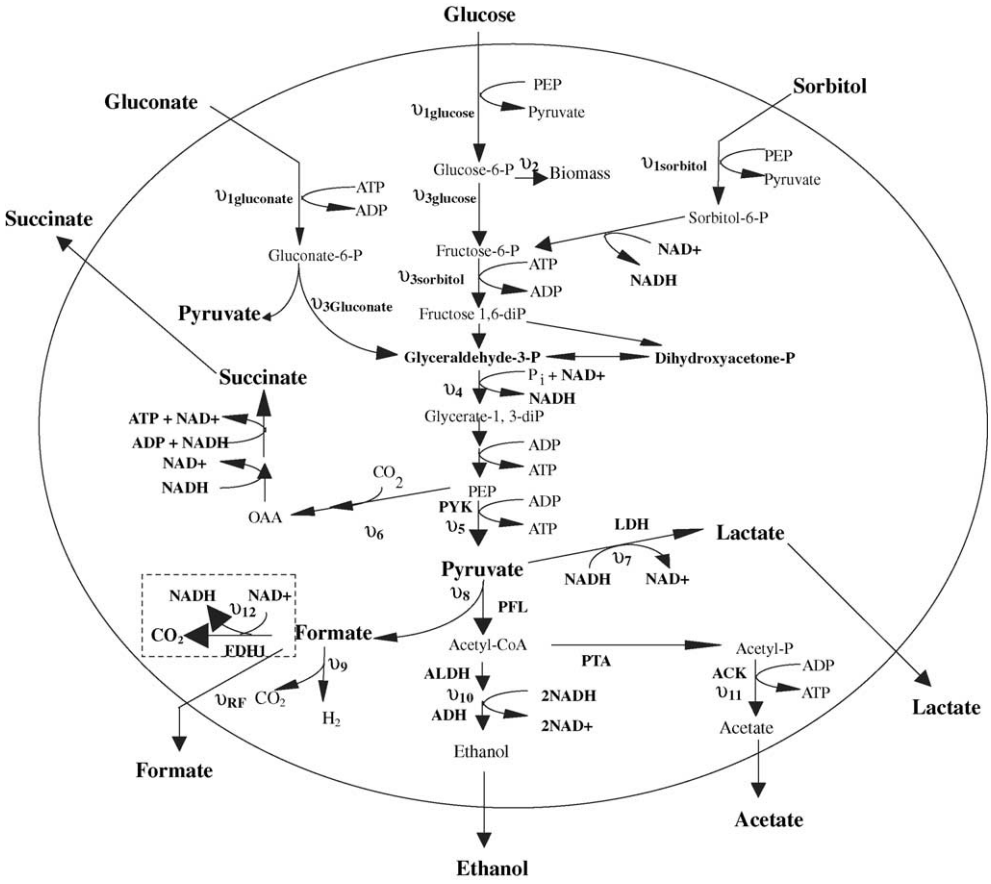

Fig. 1. Central anaerobic metabolic pathway of *E. coli*. The generation of NADH, regeneration of NAD^+, including the NAD^+-dependent formate dehydrogenase (FDH) from *Candida boidinii*, and the differences in the oxidation of glucose, sorbitol and gluconate as they enter into glycolysis are shown. The heterologous FDH pathway is shown in bold arrows and inside the dotted-line box. Note differences in NADH production. The fluxes through each pathway are designated υ_1–υ_{12}.

dehydrogenase (FDH) from *Candida boidinii* in *E. coli*. This NAD^+-dependent FDH pathway converts 1 mol of formate into 1 mol of NADH and carbon dioxide (Fig. 1). In contrast, the native FDH converts formate to CO_2 and H_2 with no cofactor involvement. The NAD^+-dependent FDH system allows the cells to retain the reducing power that otherwise will be lost by release of formate or hydrogen in the native pathway. This NADH regeneration system doubled the maximum yield of NADH from glucose from 2 to 4 mol NADH/mol substrate consumed in complex medium. In the case where sorbitol (a sugar more reduced than glucose) was used as a carbon source, a NADH yield of 4.6 mol NADH/mol substrate was obtained using complex medium under batch conditions (Berríos-Rivera et al., 2004). The higher NADH availability significantly changed the final metabolite concentration pattern under anaerobic conditions.

The current study examines the effect of a range of NADH availability levels on the distribution of metabolic fluxes in *E. coli* using defined medium in chemostat cultures. Different levels of NADH availability were achieved by combining two strategies of cofactor manipulation, namely feeding carbon sources with different oxidation state and regenerating NADH by means of the NAD^+-dependent FDH pathway. This study examines the effect of these different combinations on the NADH availability and on the distribution of metabolic fluxes, intracellular levels of NADH and NAD^+, NADH/NAD^+ ratio and total levels of NAD(H/$^+$) in *E. coli*.

2. Material and methods

2.1. Bacterial strains and plasmids

The bacterial strains and plasmids used in this study are listed in Table 1. Plasmid pSBF2 contains the *fdh1* gene from the yeast *C. boidinii* under the control of the lac promoter (Berríos-Rivera et al., 2002b). Strain GJT001 was transformed with pSBF2 and with pDHK29 to serve as negative control.

2.2. Inoculum preparation

Five milliliters of LB with the 100 mg/L of kanamycin was inoculated with 5–10 μL of the glycerol stock. This culture was grown at 37 °C and 250 rpm in a rotary shaker for 8–12 h. Then, 100 μL of the 5-ml culture was transferred to 50 mL of LB in a 250 ml shake flask with 100 mg/L of kanamycin, and grown at 37 °C and 250 rpm for 8–12 h. A 40 mL volume of this culture was centrifuged and resuspended in 6 mL of LB medium and used to inoculate the bioreactor. The inoculum constituted 1% of the liquid volume in the bioreactor.

Table 1
List of strains and plasmids

	Significant genotype	References
Strains		
GJT001	Laboratory wild type spontaneous *cadR* mutant of MC4100, Sm^R	Tolentino et al. (1992)
Plasmids		
pSBF2	*fdh1* from yeast *Candida boidinii* in pDHK30, Km^R	Berríos-Rivera et al. (2002b)
pDHK29	Control vector, Km^R	Phillips et al. (2000)

2.3. Medium

Defined medium supplemented with 20 g/L of glucose, sorbitol or gluconate was used for the chemostat runs. To reduce the initial lag time that occurs under anaerobic conditions, 1 g/L $NaHCO_3$ was added to the defined medium. The medium was also supplemented with 100 mg/L of kanamycin and 30 μL/L antifoam 289 (Sigma). The defined medium consisted of 7 g/L Na_2HPO_4, 3 g/L KH_2PO_4, 0.5 g/L NaCl and 1 g/L NH_4Cl. This salt mixture was autoclaved and then supplemented with filter–sterilized solutions of thiamine, $MgSO_4$ and $CaCl_2$, which were added to a final concentration of: 6 μg/L, 0.1 mM and 0.1 mM, respectively.

2.4. Bioreactor conditions

The fermentations were conducted under anaerobic chemostat conditions at a dilution rate of 0.05 h^{-1}. A 1-L bioreactor (New Brunswick Scientific, Bioflo 110) was used. It initially contained 0.6 L of medium during the anaerobic batch stage and then was maintained at this same working volume for the anaerobic chemostat

stage. The pH, temperature and agitation were maintained at 7.0, 32 °C and 250 rpm, respectively. A constant flow of nitrogen (3 mL/min) was maintained in the fermentor headspace to establish anaerobic conditions. The continuous culture reached steady state after 4–6 residence times. Samples were taken during the steady-state phase.

2.5. Analytical techniques

The cell density, the measurement of the concentration of metabolites and the analysis of the gas composition of the chemostat runs were described previously (Berríos-Rivera et al., 2002c). The enzymatic assay for FDH activity and the measurement of the intracellular concentration of NADH and NAD^+ were performed as described previously (Berríos-Rivera et al., 2002c). One unit was defined as the amount of enzyme that produced 1 μmol of NADH/min at 30 °C.

3. Results

The main purpose of this study is to explore the effect of a range of NADH availability levels on the distribution of metabolic fluxes in *E. coli* under anaerobic chemostat conditions using defined medium. Experiments were conducted using carbon sources with different oxidation states (gluconate (+1), glucose (0) and sorbitol (−1); the oxidation state is shown in parenthesis beside the carbon source) and with strains GJT001(pDHK29) and GJT001(pSBF2). The use of defined medium provides a cleaner characterization of the mechanism utilized by *E. coli* to achieve a redox balance under different levels of NADH supplementation, avoiding the possible interference or complication caused by the extra reducing power derived from the yeast extract and tryptone contained in the complex medium. A chemostat mode was chosen because it allows the determination of the concentrations of NADH, NAD^+ and the metabolic fluxes at steady state. It also allows fixing the specific growth rate of each strain by fixing the dilution rate ($0.05\ h^{-1}$), which will provide a precise comparison among the various strains and carbon sources.

Fig. 2 shows the steady-state specific metabolic fluxes of various metabolites in mmol/(g dry weight (D.W.) h) and the NADH utilized for the formation of reduced metabolites (succinate, lactate and ethanol) per carbon source consumed (NADH/CS). The metabolic fluxes of acetate and lactate decreased with increased NADH availability, while the ethanol showed an opposite trend; it increased with increased NADH availability.

The specific acetate formation rates of the FDH bearing strain, GJT001(pSBF2), was lower than that of the control strain, GJT001(pDHK29), for all three carbon sources studied. The control strain, GJT001(pDHK29), yielded the highest acetate production rate when grown in gluconate, which was about six times that of the lowest value given by GJT001(pSBF2), when grown in sorbitol. When glucose was used as a carbon source, the specific rate of acetate dropped by more than half in the presence of the NAD^+-dependent FDH (Fig. 2). Both, the type of carbon source and the presence of the heterologous FDH, have a much more pronounced effect on the specific lactate formation rate. The specific lactate formation rate was the highest (about 0.5 mmol/g D.W. h) for the control strain grown in gluconate, but dropped to less than 0.1 mmol/g D.W. h for the NAD^+-dependent FDH strain when grown in the same carbon source (Fig. 2). The specific lactate formation rate, however, was below 0.1 mmol/g D.W. h when grown in glucose, with and without the heterologous FDH. Finally, the lactate concentration was below the detectable level (<0.1 mM) for the culture grown in sorbitol, with and without the heterologous FDH.

Cultures grown in gluconate had a very low specific ethanol formation rate; the presence of the NAD^+-dependent FDH increased the rate only slightly (Fig. 2). The FDH strain, GJT001(pSBF2), however gave the highest ethanol production rate when grown in sorbitol, reaching to a value of about 8 mmol/g D.W. h, which was about twice that of the control strain grown in glucose.

The specific carbon source uptake rate of the control strain, GJT001(pDHK29), is the highest when grown in gluconate but decreases for both glucose and sorbitol. The presence of the NAD^+-dependent FDH lowered the specific glucose and gluconate uptake rates by about 20%. However, the sorbitol uptake rate of the NAD^+-dependent FDH bearing strain was more than 30% higher than that of the control strain, channeling the increased carbon flux to ethanol formation (Fig. 2).

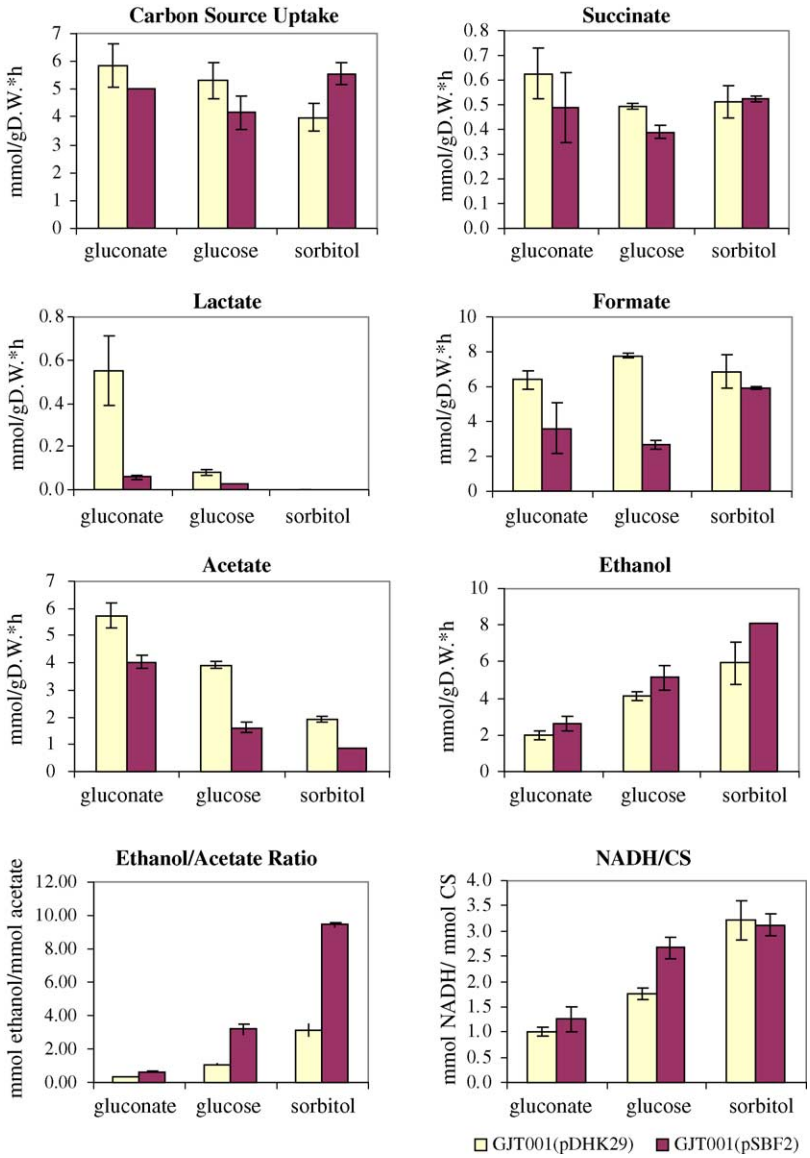

Fig. 2. Metabolic fluxes of anaerobic chemostat cultures on defined medium. The values are averaged three steady-state samples at $D = 0.05\ h^{-1}$. The error bars represent standard deviations. The metabolic fluxes are expressed in mmol/(g D.W. h). NADH/CS correponds to the experimental NADH yield. The averaged cell dry weight values of triplicate samples for GJT001(pDHK29) are 0.15, 0.09 and 0.14 g/L and for GJT001(pSBF2) are 0.15, 0.34 and 0.17 for gluconate, glucose and sorbitol, respectively.

The metabolic fluxes of succinate did not change significantly but the metabolic fluxes of residual formate decreased with the overexpression of the NAD^+-dependent FDH as expected. The formate flux of GJT001(pSBF2) in sorbitol was not significantly reduced by the presence of the heterologous FDH (Fig. 2).

Table 2 presents the theoretical and experimental values of a range of NADH availability obtained by combining the use of carbon sources with different oxidation state with or without overexpression of NAD^+-dependent FDH. The theoretical NADH yields ($Y_{(NADH)_T}$) were estimated based on the pathways

Table 2
NADH availability, ethanol yield and ethanol/acetate ratio of various strains from anaerobic chemostat experiments

Strain	Carbon source	$Y_{(NADH)_T}$ [a] (mol/mol)	$(NADH)_U/CS$ [b] (mol/mol)	$Y_{(ethanol)}$ (mol/mol)	Ethanol/acetate	FDH activity (U/mg)
GJT001(pDHK29)	Gluconate	1	1.02	0.31	0.35	ND
	Glucose	2	1.77	0.78	1.05	ND
	Sorbitol	3	3.21	1.56	3.09	ND
GJT001(pSBF2)	Gluconate	3	1.26	0.49	0.65	0.50 ± 0.02
	Glucose	4	2.67	1.23	3.18	0.26 ± 0.07
	Sorbitol	5	3.11	1.46	9.45	0.27 ± 0.04

[a] The theoretical NADH ($Y_{(NADH)_T}$) values were estimated based on the pathways shown in Fig. 1 and equals the moles of NADH produced from the oxidation of the carbon source and the conversion of formate through the NAD^+-dependent FDH pathway per mole of carbon source consumed. For the FDH strain it was assumed that all carbon will go through the PFL pathway yielding two extra moles of NADH per mole of carbon consumed.

[b] The experimental NADH ($NADH_U/CS$) values were estimated stoichiometrically from the concentrations of reduced metabolites by calculating the NADH used for their production per mole of carbon source, where $NADH_U$ is the total NADH used for product formation per unit volume (mol/L) and CS the concentration of carbon source consumed (mol/L).

shown in Fig. 1. In the calculation of the theoretical NADH yield for the FDH strain, it was assumed that all carbon went through the PFL pathway generating two extra moles of NADH per mole of carbon source consumed. $Y_{(NADH)_T}$ ranged from 1 to 5 mol NADH/CS while the experimental values ranged from 1.02 to 3.11. The ethanol yield and the Et/Ac ratio positively correlated with NADH availability. The NADH yields for the strain with the heterologous FDH were far from the theoretical yield but still were slightly higher than the control strain in each carbon source studied except for sorbitol.

Table 3 presents the results as calculated metabolic fluxes in mmol/(g D.W. h) represented as υ_1–υ_{12} according to Fig. 1. Note that υ_{12} represents the newly added NAD^+-dependent FDH pathway. Additionally, υ_{RF} represents the flux of residual formate excreted to the media based on HPLC measurements. The metabolic fluxes with an asterisk were calculated based on measured metabolites, while the other fluxes were estimated based on the relationships shown in Fig. 1, the law of mass conservation, and the pseudo-steady-state hypothesis (PSSH) on the intracellular intermediate metabolites as described in previous work (Aristidou et al., 1999; Yang et al., 1999). This table also includes the ATP net conversion defined as $\Gamma_{ATP} = -\upsilon_1 + \upsilon_4 + \upsilon_5 + \upsilon_{11} + \upsilon_6$ for gluconate and $\Gamma_{ATP} = 3\upsilon_3 + \upsilon_{11}$ for glucose and sorbitol; the NADH formation rate defined as $\Gamma_{(NADH)_f} = \upsilon_4 + \upsilon_{12}$ for gluconate and glucose; and $\Gamma_{(NADH)_f} = \upsilon_1 + \upsilon_4 + \upsilon_{12}$ for sorbitol; and the NADH utilization rate defined as $\Gamma_{(NADH)_u} = 2\upsilon_6 + \upsilon_7 + 2\upsilon_{10}$. In addition, Table 3 presents the flux of formate converted to CO_2 through both the native FDH pathway (υ_9) and the new NAD^+-dependent FDH pathway (υ_{12}) for both strains in each carbon source. The flux to formate was obtained based on the assumption that 1 mol of formate is produced per mole of acetyl-CoA formed through PFL (Fig. 1) as described in Berríos-Rivera et al. (2002c).

The glycolytic pathway (υ_1, υ_3–υ_5) decreased with NAD^+-dependent FDH overexpression in gluconate and glucose resulting in a decreased flux through the PFL to formate (υ_8). These results are in contrast with the behavior observed in complex medium where glucose uptake rate increased with overexpression of the new FDH pathway (Berríos-Rivera et al., 2002c). The flux through the native FDH to H_2 (υ_9) decreased with decreasing oxidation state of carbon source and also with the expression of the NAD^+-dependent FDH except for GJT001(pSBF2) in gluconate where the H_2 levels were below the detection limit. The ATP net flux decreased with overexpression of the NAD^+-dependent FDH and this is consistent with the observed decrease in glycolytic fluxes and acetate flux. The flux through the NAD^+-dependent pathway (υ_{12}) was many fold higher than the flux through the native FDH pathway indicating that the new pathway competes effectively with the native FDH pathway in agreement with previous results in complex medium (Berríos-Rivera et al., 2002b). The CO_2 formation would also be expected to increase as a result of an increase in υ_{12}.

Table 3
Effect of heterologous NAD^+-dependent FDH on metabolic flux distribution for anaerobic chemostat cultures in defined medium supplemented with 20 g/L of glucose

Flux or rate	To	GJT001(pDHK29)			GJT001(pSBF2)		
		Gluconate	Glucose	Sorbitol	Gluconate	Glucose	Sorbitol
υ_1	CS uptake*	4.77[b]	5.31	3.99	3.94[b]	4.16	5.55
υ_2	Biosynthesis	0.68	0.99	0.00	0.68	0.58	0.81
υ_3	G-3-P	4.77	4.31	4.17	3.94	3.58	4.74
υ_4	PEP	4.09	8.63	8.35	3.26	7.15	9.49
υ_5	Pyruvate	3.47	8.13	7.84	2.78	6.76	8.96
υ_6	Succinate*	0.63	0.49	0.51	0.49	0.39	0.52
υ_7	Lactate*	0.55	0.08	0.00	0.06	0.02	0.00
υ_8	Formate	7.69	8.05	7.84	6.66	6.74	8.96
υ_9	H_2*	0.67	0.55	0.26	BDL	0.21	0.19
υ_{RF}	Residual formate*	6.38	7.78	6.87	3.60	2.68	5.92
υ_{10}	Ethanol*	1.96	4.13	5.93	2.63	5.13	8.10
υ_{11}	Acetate*	5.73	3.93	1.92	4.03	1.61	0.86
υ_{12}	New FDH pathway[a]	0.00	0.00	0.00	3.06	3.85	2.85
Γ_{ATP}	ATP net conversion	9.15	16.86	14.44	6.62	12.34	15.09
$\Gamma_{(NADH)_f}$	NADH formation	4.09	8.63	12.34	6.32	11.00	17.89
$\Gamma_{(NADH)_u}$	NADH utilization	5.72	9.32	12.86	6.29	11.06	17.26
Γ_{CO_2}	CO_2 net conversion	0.04	0.06	0.00	2.58	3.67	2.51

Note: Metabolic fluxes in mmol/(g D.W. h) at $D = 0.05\ h^{-1}$ are represented as υ_1–υ_{12} as shown in Fig. 1. Metabolic fluxes with an asterisk (*) were calculated based on measured metabolites, while the other fluxes were estimated from the measured metabolites based on relationships shown in Fig 1. The metabolic matrix is constructed on the basis of the law of mass conservation and of the pseudo-steady-state hypothesis (PSSH) of the intracellular metabolites. G-3-P, glyceraldehyde 3-phosphate; PEP, phosphoenolpyruvate; biosynthesis, carbon assumed to be converted to biomass from glucose not fermented to fermentation products.

[a] New FDH pathway: newly added NAD^+-dependent FDH pathway; BDL: below detection limit.

[b] Gluconate uptake rates were estimated from carbon balance.

The acetyl-CoA branch partitioning commits carbon flux toward ethanol or acetate production. The partitioning of fluxes toward ethanol and acetate is 50–50% in cultures of the control strain in glucose; this is an ethanol/acetate ratio of one. In an effort to achieve proper redox balance the ethanol flux increased with decreased acetate flux to compensate for increased NADH availability. Table 2 shows the Et/Ac ratio obtained for both strains in each carbon source. These values are slightly lower than those previously reported in batch experiments (Berríos-Rivera et al., 2004). The observed Et/Ac ratio in glucose of both strains very similar to the results obtained in chemostat cultures using complex medium, in general the metabolite distribution was similar in both complex and defined medium; however, higher fluxes were seen in complex medium (Berríos-Rivera et al., 2004c). The control strain in glucose exhibits an Et/Ac ratio of 1.05 and this ratio increased to 3.09 when cultivated in sorbitol, and decreased to 0.34 when gluconate was used. The highest Et/Ac ratio (9.45) was obtained by combining sorbitol as a carbon source with the strain overexpressing the NAD^+-dependent FDH.

Table 3 also shows the NADH formation and utilization rates ($\Gamma_{(NADH)_f}$ and $\Gamma_{(NADH)_u}$). The NADH formation and utilization rates were very similar for every case studied and these rates increased with increased NADH availability.

Fig. 3 shows the steady-state concentrations of $NAD(H/^+)$ and the total $NAD(H/^+)$ in μmol/g D.W. and the $NADH/NAD^+$ ratio. The intracellular NADH increased with overexpression of the NAD^+-dependent FDH relative to the control strain in each of the carbon sources examined. The intracellular NADH concentrations ranged between 1 and 2 μmol/g D.W., with 1 being the lowest concentration obtained for the control strain on gluconate and 2 being the concentration obtained for the FDH–sorbitol combination. The NAD^+ concentrations ranged between

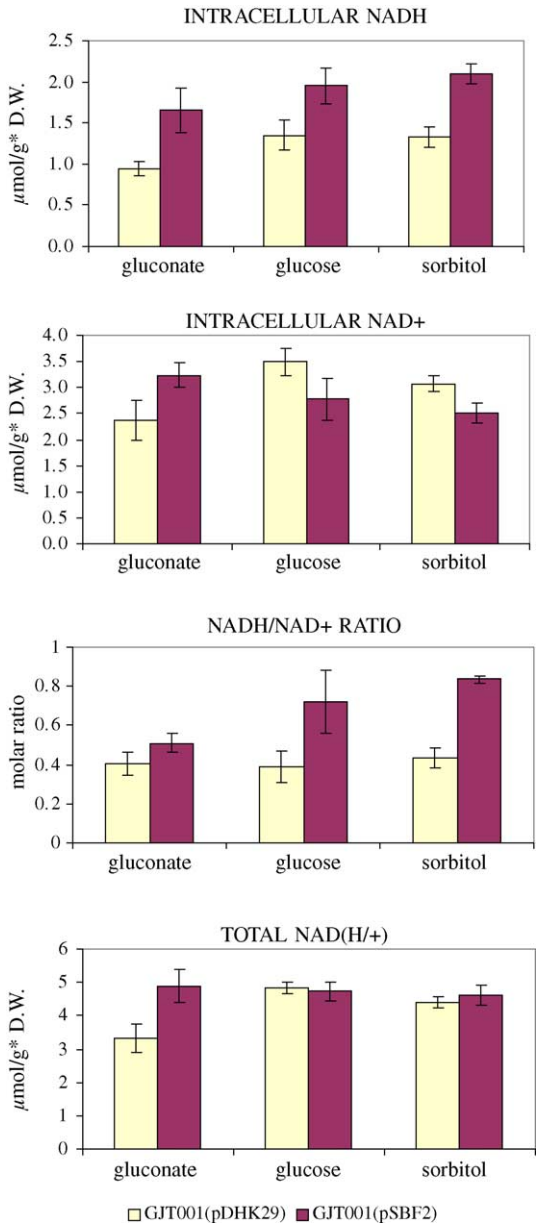

Fig. 3. Anaerobic chemostat data on intracellular NAD(H/$^+$) parameters. The NAD$^+$ and NADH concentrations are expressed in μmol/g D.W. The values are averaged three steady-state samples at $D = 0.05\,h^{-1}$. The error bars represent standard deviations.

2.4 and 3.5 μmol/g D.W. The overexpression of the NAD$^+$-dependent FDH increased the NADH/NAD$^+$ ratio for each of the carbon sources examined relative to the control strain. Additionally, the ratio increased slightly for glucose and sorbitol relative to gluconate for GTJ001(pSBF2), while for the control strain the NADH/NAD$^+$ ratio obtained in different carbon sources remain unchanged. The results showed that genetic manipulation changed the equilibrium concentration of these cofactors to a new equilibrium value.

4. Discussion

Strain GJT001(pSBF2) contains the NAD$^+$-dependent formate dehydrogenase (FDH) from *C. boidinii* (Berríos-Rivera et al., 2002b). This NAD$^+$-dependent FDH pathway converts 1 mol of formate into 1 mol of NADH and carbon dioxide. Strain GJT001(pDHK29) was used as a control, harboring solely the cloning vector.

The overexpression of the NAD$^+$-dependent FDH significantly changed the distribution of the metabolic fluxes in *E. coli*. These observations are consistent with previously reported results under anaerobic chemostat cultures using complex media (Berríos-Rivera et al., 2002c). One of the most relevant results observed is the shift in ethanol to acetate ratio (Et/Ac), which indicates an increase in intracellular NADH availability. This ratio increased from 0.34 ± 0.01 for the control strain cultivated in gluconate to 9.45 ± 0.18 for the strain with the NAD$^+$-dependent FDH in sorbitol (Fig. 2; Table 2). These results reveal that the NADH availability increases with the decrease in oxidation state of the carbon source and with the overexpression of the NAD$^+$-dependent FDH. The overexpression of the NAD$^+$-dependent FDH decreased carbon consumption as opposed to results in complex media where the carbon consumption was increased by the NAD$^+$-dependent FDH expression. In the case of the NAD$^+$-dependent FDH–sorbitol combination, sorbitol consumption was increased in the presence of the NAD$^+$-dependent FDH relative to its control.

The metabolic fluxes of acetate and lactate decreased with increased NADH availability, while the ethanol increased with increased NADH availability. The yields for these metabolites also follow a similar trend; the ethanol yield also increased with increased NADH availability except for the case of the NAD$^+$-dependent FDH–sorbitol combination where

the ethanol yield remained almost the same as the yield achieved by the control strain on sorbitol, 1.5 mol Et/mol sorbitol. These results suggest that somehow the NAD^+-dependent FDH–sorbitol combination might be saturated by excess NADH, and is not capable of recycling any further the extra NADH through the production of ethanol. This idea is supported by a decreased flux observed through the new FDH pathway compared to gluconate and glucose (see Table 3). It is also possible that this combination would be more beneficial for the production of a compound more reduced than ethanol.

It is important to mention that the metabolic fluxes were much smaller in defined medium compared to previous studies of the same strains on complex medium (Berríos-Rivera et al., 2002c). However, the Et/Ac ratio and the NADH utilized for the formation of reduced metabolites were very similar suggesting an effort of the cells to achieve a similar redox state in both defined medium and complex medium.

The metabolic fluxes of residual formate decreased with the overexpression of the NAD^+-dependent FDH as expected. For the NAD^+-dependent FDH–sorbitol case, the formate flux was not significantly reduced. This observation suggests that the rate of formate usage is small compared to the rate of formate formation, which may be due to an excess NADH availability. This observation is also in agreement with the finding that the ethanol yield and NADH/CS could not be further increased relative to the control-sorbitol system. As seen in Fig. 2, the NADH/CS increases with the oxidation state of the carbon source and with the overexpression of the NAD^+-dependent FDH, but no further increase was observed for the NAD^+-dependent FDH–sorbitol combination. The chemostat values of NADH/CS shown in Table 2 were slightly lower than the values obtained previously in anaerobic tube experiments using defined medium (Berríos-Rivera et al., 2004), and this variation can be attributed to the differences in cultivation conditions.

An analysis of the metabolic fluxes obtained here compared to previous complex medium chemostat cultures (Berríos-Rivera et al., 2002c) shows that the mechanism of redistribution utilized by the cells in order to achieve a redox state is different. In complex medium, the Et/Ac ratio was adjusted by mainly controlling the flux through the ethanol pathway; thus, as the NADH availability increased the ethanol flux increased accordingly and no significant change in the acetate flux was observed. In defined medium the Et/Ac ratio was adjusted by regulating both, the flux through ethanol and acetate. Comparing the strain with the NAD^+-dependent FDH relative to its control strain in each of the carbon sources examined, it is observed that the acetate flux decreased as the ethanol flux was increased; in general it was found that the decrease in acetate was more dramatic than the increase in ethanol. A possible reason for the difference in the cells mechanism to achieve a redox balance could be that in complex medium extra reducing power could potentially be used to increase the amounts of reduced by-product and its yield while in defined medium by-product formation is limited only to the NADH that can be supplied by the carbon source.

The NADH formation rates and NADH utilization rates, presented in Table 3, were very similar in each individual case. These results suggest that most of the NADH formed through the oxidation of the carbon source and the new FDH degradation pathway can be accounted for as being utilized for the formation of reduced metabolites, specifically, succinate, lactate and ethanol. The biomass formation rates shown in Table 3 were small; therefore, the fraction of the NADH utilization rate to generate biomass is negligible.

Table 4 presents the calculated yields for different fermentation products in C-mole produced per C-mole of glucose consumed. The normalized data present the results in a more informative manner. Using glucose as the base case, we observed that for strain GJT001(pDHK29), the carbon is distributed equally to ethanol (0.26) and acetate (0.25), the rest of the carbon goes mostly to formate, while lactate and succinate constitute only minor products. The general trends are that when the new FDH is overexpressed lactate, acetate and residual formate decreases, while the ethanol and formate converted increase; the same effect is observed in lactate and acetate when a more reduced carbon source is used within a same strain. The combined effect seems to be additive, as seen by cultures expressing the heterologous FDH in sorbitol, where the acetate carbon yield drops to 0.05. The ethanol yield could not increase further using this combination suggesting that the cells are unable to handle excess NADH.

Table 4
Distribution of metabolites from 1 carbon-mole of gluconate, glucose or sorbitol uptaken by the cell

Metabolite	Carbon source		
	Gluconate	Glucose	Sorbitol
Succinate			
GJT001(pDHK29)	0.05	0.05	0.07
GJT001(pSBF2)	0.05	0.05	0.05
Lactate			
GJT001(pDHK29)	0.05	0.01	0.00
GJT001(pSBF2)	0.01	0.00	0.00
Formate			
GJT001(pDHK29)	0.22	0.25	0.35
GJT001(pSBF2)	0.22	0.27	0.27
Formate converted			
GJT001(pDHK29)	0.04	0.01	0.04
GJT001(pSBF2)	0.10	0.16	0.09
Residual formate			
GJT001(pDHK29)	0.18	0.24	0.30
GJT001(pSBF2)	0.12	0.11	0.18
Acetate			
GJT001(pDHK29)	0.33	0.25	0.17
GJT001(pSBF2)	0.27	0.13	0.05
Ethanol			
GJT001(pDHK29)	0.11	0.26	0.52
GJT001(pSBF2)	0.18	0.41	0.49

Values shown are averaged triplicate steady-state yields in C-mole produced per C-mole of carbon source consumed. Results were obtained from anaerobic chemostat cultures using defined medium at $D = 0.05\,h^{-1}$.

5. Intracellular concentration of NAD(H/$^+$) at steady state

The intracellular NADH levels measured in strain GJT001(pSBF2) were significantly higher than the levels found in GJT001(pDHK29) ($P < 0.05$) (Fig. 3). Additionally, we also observed a significant difference in NADH values due to the effect of the carbon source ($P < 0.05$). In particular, the control strain in gluconate had the lowest NADH value with respect to glucose and sorbitol. The NAD^+ levels were not significantly different between strains nor between carbon sources ($P < 0.05$) suggesting that any changes in the $NADH/NAD^+$ ratio can be attributed mainly to increased intracellular NADH levels.

The $NADH/NAD^+$ ratio changed both, due to the NAD^+-dependent pathway incorporation and due to carbon source used. Specifically, we observed differences due to strain effect in glucose and sorbitol and the carbon source effect was significant when comparing gluconate with respect to glucose and sorbitol in the strain with the NAD^+-dependent FDH. The $NADH/NAD^+$ ratio was similar for the control strain in the three carbon sources examined suggesting that the cells are able to adjust the turnover of the NADH pool fast in an effort to attain a redox balance.

The total NAD ($H/^+$) levels were very similar for all the strains examined in different carbon sources except for the control strain on gluconate, which showed lower total levels than the rest.

Acknowledgement

This work was supported by the National Science Foundation (BES000030).

References

Alam, K.Y., Clark, D.P., 1989. Anaerobic fermentation balance of *Escherichia coli* as observed by in vivo nuclear magnetic Resonance spectroscopy. J. Bacteriol. 171, 6213–6217.

Aristidou, A.A., San, K.-Y., Bennett, G.N., 1999. Metabolic flux analysis of *Escherichia coli* expressing the *Bacillus subtilis* acetolactate synthase in batch and continuous cultures. Biotechnol. Bioeng. 63, 737–749.

Berríos-Rivera, S. J. (2002a). Metabolic engineering of cofactors ($NADH/NAD^+$) in *Escherichia coli*. Ph.D. Thesis. Rice University, Houston, TX.

Berríos-Rivera, S.J., Bennett, G.N., San, K.-Y., 2002b. Metabolic engineering of *Escherichia coli*: increase of NADH availability by overexpressing an NAD^+-dependent formate dehydrogenase. Metab. Eng. 4, 217–229.

Berríos-Rivera, S.J., Bennett, G.N., San, K.-Y., 2002c. The effect of increasing NADH availability on the redistribution of metabolic fluxes in *Escherichia coli* chemostat cultures. Metab. Eng. 4, 230–237.

Berríos-Rivera, S.J., San, K.-Y., Bennett, G.N., 2002d. The effect of NAPRTase overexpression on the total levels of NAD, the $NADH/NAD^+$ ratio, and the distribution of metabolites in *Escherichia coli*. Metab. Eng. 4, 238–247.

Berríos-Rivera, S.J., San, K.-Y., Bennett, G.N., 2003. The effect of carbon sources and lactate dehydrogenase deletion on 1,2-propanediol production in *Escherichia coli*. J. Ind. Microbiol. Biotechnol. 30, 34–40.

Berríos-Rivera, S.J., Sánchez, A.M., Bennett, G.N., San, K.-Y., 2004. Effect of different levels of NADH availability on metabolite distribution in *Escherichia coli* fermentation in defined and complex media. App. Microbiol. Biotechnol. 65, 426–432.

Clark, D.P., 1989. The fermentation pathways of *Escherichia coli*. FEMS Microbiol. Lett. 63, 223–234.

De Graef, M.R., Alexeeva, S., Snoep, J.L., Teixeira de Mattos, M.J., 1999. The steady-state internal redox state (NADH/NAD) reflects the external redox state and is correlated with catabolic adaptation in *Escherichia coli*. J. Bacteriol. 181, 2351–2357.

Phillips, G.J., Park, S.-K., Huber, D., 2000. High copy number plasmids compatible with commonly used cloning vectors. BioTechniques 28, 400–408.

San, K.-Y., Bennett, G.N., Berríos-Rivera, S.J., Vadali, R.V., Yang, Y.T., Horton, E., Rudolph, F.B., Sariyar, B., Blackwood, K., 2002. Metabolic engineering through cofactor manipulation and its effects on metabolic flux redistribution in *Escherichia coli*. Metab. Eng. 4, 182–192.

Tolentino, G.J., Meng, S.-Y., Bennett, G.N., San, K.-Y., 1992. A pH-regulated promoter for the expression of recombinant proteins in *Escherichia coli*. Biotechnol. Lett. 14, 157–162.

Yang, Y.-T., Aristidou, A.A., San, K.-Y., Bennett, G.N., 1999. Metabolix flux analysis of *Escherichia coli* deficient in the acetate production pathway and expressing the *Bacillus subtilis* acetolactate synthase. Metab. Eng. 1, 26–34.